Metabolic Engineering 70 (2022) 102–114

Contents lists available at ScienceDirect

Metabolic Engineering

journal homepage: www.elsevier.com/locate/meteng

Secretory production of spider silk proteins in metabolically engineered *Corynebacterium glutamicum* for spinning into tough fibers

Qing Jin [a,1], Fang Pan [a,1], Chun-Fei Hu [a], Sang Yup Lee [b], Xiao-Xia Xia [a,*], Zhi-Gang Qian [a,**]

[a] *State Key Laboratory of Microbial Metabolism, Joint International Research Laboratory of Metabolic & Developmental Sciences, and School of Life Sciences and Biotechnology, Shanghai Jiao Tong University, 800 Dongchuan Road, Shanghai, 200240, People's Republic of China*

[b] *Metabolic and Biomolecular Engineering National Research Laboratory, Department of Chemical & Biomolecular Engineering (BK21 Four Program), BioProcess Engineering Research Center, Bioinformatics Research Center, and Institute for the BioCentury, KAIST, Yuseong-gu, Daejeon, Republic of Korea*

ARTICLE INFO

Keywords:
Spider dragline silk
Corynebacterium glutamicum
Spidroin
Secretion
Metabolic engineering
Fiber spinning

ABSTRACT

Spider dragline silk is a remarkable fiber made of unique proteins—spidroins—secreted and stored as a concentrated aqueous dope in the major ampullate gland of spiders. This feat has inspired engineering of microbes to secrete spidroins for spinning into tough synthetic fibers, which remains a challenge due to the aggregation-prone feature of the spidroins and low secretory capacity of the expression hosts. Here we report metabolic engineering of *Corynebacterium glutamicum* to efficiently secrete recombinant spidroins. Using a model spidroin MaSpI16 composed of 16 consensus repeats of the major ampullate spidroin 1 of spider *Trichonephila clavipes*, we first identified the general Sec protein export pathway for its secretion via N-terminal fusion of a translocation signal peptide. Next we improved the spidroin secretion levels by selection of more suitable signal peptides, multiplexed engineering of the bacterial host, and by high cell density cultivation of the resultant recombinant strains. The high abundance (>65.8%) and titer (554.7 mg L^{-1}) of MaSpI16 in the culture medium facilitated facile, chromatography-free recovery of the spidroin with a purity of 93.0%. The high solubility of the purified spidroin enabled preparation of highly concentrated aqueous dope (up to 66%) amenable for spinning into synthetic fibers with an appreciable toughness of 70.0 MJ m^{-3}. The above metabolic and processing strategies were also found applicable for secretory production of the higher molecular weight spidroin MaSpI64 (64 consensus repeats) to yield similarly tough fibers. These results suggest the good potential of secretory production of protein polymers for sustainable supply of fibrous materials.

1. Introduction

Spider dragline silk exhibits extraordinary mechanical properties such as high tensile strength and extensibility that make it tougher than nearly all other natural and synthetic materials (Chung et al., 2012; Omenetto and Kaplan, 2010). The main components of dragline silk are major ampullate spidroins I (MaSpI) and II (MaSpII), proteins that are named after their secreting gland. Their molecular weights are high at 250−320 kDa (Ayoub et al., 2007; Kono et al., 2021; Sponner et al., 2005). These silk proteins (spidroins) comprise a long repetitive core region flanked by nonrepetitive amino- and carboxy-termini of about 100 amino acid residues (Ayoub et al., 2007). The repetitive region is rich in polyalanine and polyglycine motifs, and the polyalanine motifs enables the formation of crystalline β-sheet structures responsible for the high strength of dragline silk, whereas the glycine-rich motifs contribute to the extensibility and flexibility of the silk fibers (Gatesy et al., 2001; Heim et al., 2009; Oktaviani et al., 2018).

The demand for spider dragline silk is increasing for diverse applications due to its extraordinary mechanical and physiochemical properties (Omenetto and Kaplan, 2010; Qin et al., 2021; Zhou et al., 2018). However, sustainable supply of natural dragline silk is not practical by farming spiders because they are territorial and produce small amounts of the silk fibers (Andersson et al., 2017; Xia et al., 2010). Therefore, it is highly desirable to produce recombinant spidroins for processing into synthetic dragline silk fibers and other forms of biomaterials (Bowen et al., 2018; Gonska et al., 2020; Jones et al., 2015; Saric et al., 2021).

* Corresponding author.
** Corresponding author.
E-mail addresses: xiaoxiaxia@sjtu.edu.cn (X.-X. Xia), zgqian@sjtu.edu.cn (Z.-G. Qian).
[1] These authors contributed equally to this work.

https://doi.org/10.1016/j.ymben.2022.01.009
Received 10 November 2021; Received in revised form 6 January 2022; Accepted 17 January 2022
Available online 20 January 2022
1096-7176/© 2022 International Metabolic Engineering Society. Published by Elsevier Inc. All rights reserved.

Many attempts have been made to produce recombinant spidroins in a variety of heterologous hosts (Chung et al., 2012; Whittall et al., 2021). The traditional approach is to accumulate recombinant silk proteins in the cytosol of bacterial or insect cells (Foong et al., 2020; Huemmerich et al., 2004; Lewis et al., 1996; Schmuck et al., 2021) or in the endoplasmic reticulum of plant leaves (Scheller et al., 2001). A major limitation of this approach is the confined cell volume leading to the difficulty in maintaining solubility of the overexpressed silk proteins, the restriction on protein yield, and extensive cell lysis and purification steps to harvest the target proteins (Huemmerich et al., 2004; Winkler et al., 2000; Wei et al., 2020; Zhang et al., 2008). Another strategy is to directly produce fibrous spider silk in the secreting-silk organs of transgenic silkworms (Kuwana et al., 2014; Teulé et al., 2012; Xu et al., 2018). The ability to assemble recombinant spider silk proteins into fibers is intriguing in these studies, yet the intrinsical production of silkworm silks restricts the amount of spider silk proteins in the transgenic silkworms and consequently the mechanical properties of the fibers. Alternatively, secretory expression systems have been developed for extracellular production of recombinant spidroins to simplify purification and maintain soluble state of the silk proteins prior to being spun into water-insoluble fibers. For example, mammalian cells have been engineered to secrete spidroins having molecular weights of 60 to 140 kDa. The fiber with the highest average toughness value of 0.895 g per denier (gpd) was derived from a 60 kDa ADF-3 silk protein (Lazaris et al., 2002). Also, two types of dragline silk proteins (ADF3 and ADF4) were secreted by the type III secretion system of Gram-negative bacterium *Salmonella enterica* (Azam et al., 2016; Metcalf et al., 2014; Widmaier et al., 2009). However, the manufacture and mechanical test of synthetic fibers using the secreted silk proteins were not reported in these studies, probably due to the low secretion titers up to 30 mg L^{-1}.

Corynebacterium glutamicum is a Gram-positive non-spore-forming facultative-anaerobic bacterium which has been widely used for industrial production of chemicals, fuels, and biopolymers (Becker et al., 2018; Cheng et al., 2019; Xu et al., 2019). Recently, *C. glutamicum* has also been recognized as an attractive host for the secretory production of recombinant proteins due to its several significant advantages: *C. glutamicum* rarely secretes endogenous proteins to the extracellular medium which is beneficial for the simple purification process and high purity of the target proteins (Yim et al., 2016); extracellular proteolytic activity is not detected (Billman-Jacobe et al., 1995); *C. glutamicum* is endotoxin-free and generally recognized as safe (Liu et al., 2015); many tools and strategies are available for genetic and metabolic engineering of *C. glutamicum* (Cho et al., 2017); it can be grown in relatively cheap media and its industrial-scale fermentation has been well established (Park et al., 2014). There have been reports on the secretory production of a few fluorescent proteins and enzymes in the gram per liter range (Teramoto et al., 2011; Watanabe et al., 2013; Yim et al., 2016). Thus, we decided to explore the potential of this industrially robust workhorse for the secretory production of spider dragline silk proteins.

In this study, we report the development of spidroin-secreting *C. glutamicum* strains by rational selection of protein export pathway and translocation signal peptides, and metabolic engineering of the bacterial host. By high cell density cultivation, the capacity of the expression system was further enhanced to secrete two model spidroins composed of 16 and 64 consensus repeats of spider *Trichonephila clavipes* (formerly *Nephila clavipes*) MaSpI. Furthermore, a facile chromatography-free process was developed to purify the secreted spidroins, which could be highly concentrated in aqueous solutions (up to 66%, w/v) for processing into synthetic fibers with appreciable mechanical properties.

2. Materials and methods

2.1. Bacterial strains and plasmids

The bacterial strains and plasmids used in this study are listed in Table 1 and Table 2. The primers used in cloning are listed in Table S1. Chemically competent cells of *E. coli* DH5α (TIANGEN Biotech, Beijing, China) were used for gene cloning. *C. glutamicum* RES167 (a restriction-deficient derivative of wild-type strain ATCC 13032) was used as the parent to make gene knockout variants for silk protein secretion. DNA manipulations were performed according to standard protocols. PrimeSTAR® Max DNA polymerase was obtained from Takara Biotechnology Co., Ltd. (Dalian, China). All the restriction enzymes and T4 DNA ligase were purchased from New England Biolabs (Ipswich, MA). Extraction of plasmid DNA from *E. coli* was performed using the Mini Plasmid purification Kit (TIANGEN Biotech, Beijing, China), and introduced into *C. glutamicum* by electroporation using a Gene Pulser (Bio-Rad, Hercules, CA). Plasmid isolation from *C. glutamicum* was carried out with the same kit except that the cells were pre-incubated in buffer P1 supplemented with 20 mg mL^{-1} lysozyme at 37 °C for 2 h before exposure to the lysis buffer P2.

Table 1
Bacterial strains used in this study.

Name	Description	Source or Refs.
E. coli		
DH5α	F^- φ80 *lacZ*ΔM15 Δ(*lacZYA-argF*) U169 *endA1 recA*1 *hsd*R17(r_k^- m_k^+) *sup*E44 λ^- *thi*-1 *gyr*A96 *rel*A1 *pho*A	TIANGEN Biotech Co., Ltd., Beijing, China
MG1655	K-12 F^- λ^- ilvG$^-$ rfb-50 rph-1	Lab stock
C. glutamicum		
RES167	ATCC 13032 Δ(*cglIM-cglIR-cglIIR*); Restriction deficient	Lab stock
JQ01	RES167 Δ*recA*	This study
JQ02	RES167 Δ*pbp1a*	This study
JQ03	RES167 Δ*sigD*	This study
JQ04	RES167 Δ*pbp1a* Δ*sigD*	This study
JQ05	RES167 Δ*pbp1a* Δ*recA*	This study

A DNA sequence encoding the MaSp1 consensus sequence of spider *T. clavipes* (GRGGLGGQGAGAAAAAGGAGQGGYGGLGSQG) was codon-optimized for favorable expression in *C. glutamicum* using Gene Designer 2.0, which is freely available at http://www.DNA20.com. The optimized DNA was purchased from Genewiz (Suzhou, China) as a synthetic gene that was cloned into the *Nde*I and *Xho*I sites of vector pET-28a4 (Wei et al., 2020). The delivered plasmid named pET28a4-I1cg was used for construction of vectors encoding synthetic silk genes of varying length. To clone the silk gene with two tandem repeats of the MaSpI consensus sequence, plasmid pET28a4-I2cg was constructed by ligating the 4, 166-bp, *Xma*I-*Spe*I fragment of pET28a4-I1cg to the 1,388-bp, *Nhe*I-*Xma*I fragment of pET28a4-I1cg. Likewise, plasmids pET28a4-I4cg, pET28a4-I8cg, pET28a4-I16cg, pET28a4-I32cg, and pET28a4-I64cg were created that encode 4-64 repeats of the consensus sequence, using the iterative polymerization strategy as described earlier (Qian et al., 2015).

Plasmids for secretory production of silk proteins in *C. glutamicum* were constructed on the classic expression vector pXMJ19. Briefly, DNA sequences encoding signal peptides were first amplified from the genomic DNA of *C. glutamicum* RES167 except that the *torA* signal sequence was amplified from *E. coli* MG1655. The amplified DNA fragments were subsequently cloned into the *Hin*dIII-*Sal*I site of pXMJ19, leading to the respective secretory vectors. The silk genes were then liberated by digesting the aforementioned pET-28a4 derivatives with restriction enzymes *Nde*I and *Bam*HI-HF, and cloned into the same sites of the above secretory vectors. In the experimental setup for screening signal peptides, the fragments encoding signal peptides of interest were PCR-amplified from the genomic DNA of *C. glutamicum* RES167, cut with *Hin*dIII and *Nde*I, and then ligated with the 8.2 kb *Nde*I-*Hin*dIII fragment of plasmid pCG2-I16cg, a vector for secretory expression of the 16-mer silk protein under the guidance of the Cg1514 signal peptide. Alternatively, the DNA fragments encoding Cg2195 and Cg3393 signal peptides were obtained by annealing the respective primer pairs (Table S1), and directly ligated with the desirable restricted fragment of plasmid pCG2-

Table 2
Bacterial plasmids used in this study.

Name	Description[a]	Source or Refs.
pET-28a(+)	Km^R, *T7* promoter, pBR322 ori, 5.4-kb	Novagen
pET-28a4	pET-28a(+) with an inserted *Bam*HI site, 5.4-kb	This study
pET28a4-I1cg	pET-28a4 harboring monomer silk gene, 5.4-kb	This study
pET28a4-I16cg	pET-28a4 harboring 16-mer silk gene, 6.9-kb	This study
pET28a4-I64cg	pET-28a4 harboring 64-mer silk gene, 11.6-kb	This study
pXMJ19	Cm^R, *tac* promoter, pBL1 ori, pUC ori, *E. coli-C. glutamicum* shuttle vector, 6.6-kb	Lab stock
pCG2	pXMJ19 harboring *cg1514* SP sequence, 6.7-kb	This study
pCG2-I16cg	pCG2 harboring 16-mer silk gene, 8.3-kb	This study
pCG3	pXMJ19 harboring *E. coli torA* SP sequence, 6.7-kb	This study
pCG3-gfp'	pCG3 harboring a synonymous gfp_{mut3} gene, 7.4-kb	This study
pCG3-I16cg	pCG3 harboring 16-mer silk gene, 8.3-kb	This study
pCG4	pXMJ19 harboring *cg0955* SP sequence, 6.7-kb	This study
pCG4-gfp'	pCG4 harboring a synonymous gfp_{mut3} gene, 7.4-kb	This study
pCG4-I16cg	pCG4 harboring 16-mer silk gene, 8.3-kb	This study
pCG5-I16cg	Derived from pCG2-I16cg with *cg0413* SP sequence, 8.3-kb	This study
pCG6-I16cg	Derived from pCG2-I16cg with *cg1109* SP sequence, 8.3-kb	This study
pCG7-I16cg	Derived from pCG2-I16cg with *cg1243* SP sequence, 8.3-kb	This study
pCG8	pXMJ19 harboring *cg2196* SP sequence, 6.7-kb	This study
pCG8-I16cg	pCG8 harboring 16-mer silk gene, 8.3-kb	This study
pCG8-I64cg	pCG8 harboring 64-mer silk gene, 13.1-kb	This study
pCG9-I16cg	Derived from pCG2-I16cg with *cg2394* SP sequence, 8.3-kb	This study
pCG11-I16cg	Derived from pCG2-I16cg with *cg2402* SP sequence, 8.3-kb	This study
pCG12-I16cg	Derived from pCG2-I16cg with *cg2585* SP sequence, 8.3-kb	This study
pCG13-I16cg	Derived from pCG2-I16cg with *cg3182* SP sequence, 8.3-kb	This study
pCG14-I16cg	Derived from pCG2-I16cg with *cg3186* SP sequence, 8.3-kb	This study
pCG15-I16cg	Derived from pCG2-I16cg with *cg0316* SP sequence, 8.3-kb	This study
pCG17-I16cg	Derived from pCG2-I16cg with *cg1087* SP sequence, 8.3-kb	This study
pCG18-I16cg	Derived from pCG2-I16cg with *cg2195* SP sequence, 8.3-kb	This study
pCG19-I16cg	Derived from pCG2-I16cg with *cg2518* SP sequence, 8.3-kb	This study
pCG20-I16cg	Derived from pCG2-I16cg with *cg2868* SP sequence, 8.3-kb	This study
pCG21-I16cg	Derived from pCG2-I16cg with *cg0470* SP sequence, 8.3-kb	This study
pCG22-I16cg	Derived from pCG2-I16cg with *cg3393* SP sequence, 8.3-kb	This study
pK19*mobsac*B	Km^R, integration vector, *oriV*, *oriT*, *sacB*, 5.7-kb	Lab stock
pK19-Δ*recA*	pK19*mobsac*B derivative containing 1-kb homology regions flanking the *C. glutamicum recA* gene, 7.7-kb	This study
pK19-Δ*pbp1a*	pK19*mobsac*B derivative containing 1-kb homology regions flanking the *C. glutamicum pbp1a* gene, 7.7-kb	This study
pK19-Δ*sigD*	pK19*mobsac*B derivative containing 1-kb homology regions flanking the *C. glutamicum sigD* gene, 7.7-kb	This study
pTetgly2	Cm^R, dual P*tet-glyVXY* cassettes, p15A ori, 5.1-kb	Yang et al. (2016)
pTRCmob	Km^R, *E. coli-C. glutamicum* shuttle vector, *oriV*, pGA1 ori, 6.4-kb	Liu et al. (2007)
pTRC-gly2	pTRCmob with P*tet-glyVXY* cassettes, 7.3-kb	This study

[a]Abbreviations: Km, kanamycin; Cm, chloramphenicol; R, resistance; SP, signal peptide.

I16cg. This resulted in a series of secretory expression plasmids, each encoding an intended signal peptide by replacement of the original Cg1514 signal peptide.

The tandem *tet-glyVXY* cassettes were amplified from plasmid pTetgly2 (Yang et al., 2016) with PrimeSTAR® Max DNA polymerase and primers pTetgly2-F and pTetgly2-R. The resulting PCR product was cut with *Sal*I, and inserted into the *Eco*RV-*Sal*I site of shuttle vector pTRCmob (Liu et al., 2007), leading to plasmid pTRC-gly2. This plasmid allows expression of the *glyVXY* genes under the constitutive *tet* promoter.

Deletion of the *recA*, *pbp1a* and *sigD* genes in *C. glutamicum* were performed as described previously (Schäfer et al., 1994). Briefly, 1-kb sequences upstream and downstream of each target gene were PCR-amplified from the genomic DNA of *C. glutamicum* RES167, fused, and cloned into the *Sal*I-*Bam*HI site of vector pK19*mobsac*B by using the In-Fusion HD Cloning Kit (Clontech Laboratories, Inc., Mountain View, CA). The resulting integration plasmids containing the kanamycin resistance and *sacB* genes were electro-transformed into *C. glutamicum* cells for chromosomal homologous recombination. Desirable gene deleted mutants were obtained by two-step selection based on kanamycin resistance and the SacB system, and further confirmed by PCR with two primers flanking each target gene.

2.2. Secretory production of silk proteins

For protein production in flask cultivation, recombinant *C. glutamicum* strains were cultivated in 250 mL flasks containing 20 mL of 38.5 g L^{-1} brain heart infusion (BHI; Qingdao Hope Bio-Technogy Co., Ltd, Qingdao, China) medium in a shaking incubator at 30 °C and 220 rpm. When necessary, antibiotics were added into the culture medium at the following concentrations: 25 mg L^{-1} of kanamycin, 10 mg L^{-1} of chloramphenicol, and 50 mg L^{-1} of nalidixic acid. When the cell optical density at 600 nm (OD_{600}) reached ~4, the cells were treated with isopropyl-β-D-thiogalactoside (IPTG; Sigma, St. Louis, MO) at 1 mM, and further cultivated for 6 h. Cell culture samples were taken and centrifuged at 13,523*g* and 4 °C for 10 min. The resulting supernatant was collected for the analysis of extracellular proteins, and the pellets were resuspended and lysed using the same buffers as described for plasmid isolation.

For protein production by high cell density cultivation (HCDC), recombinant *C. glutamicum* strains were cultivated at 30 °C in a 5 L jar bioreactor (Biotech-5JG-7000; BaoXing Bio-Engineering Equipment, Shanghai, China) containing 2 L of a semi-defined medium supplemented with 20 g L^{-1} of glucose. The semi-defined medium contains (per liter): 3 g K_2HPO_4, 1 g KH_2PO_4, 2 g urea, 10 g $(NH_4)_2SO_4$, 2 g $MgSO_4$, 0.2 mg biotin, 5 mg thiamine, 10 mg calcium pantothenate, 10 mg $FeSO_4$, 1 mg $MnSO_4$, 1 mg $ZnSO_4$, 10 mg $CaCl_2$, 2 g yeast extract, and 7 g casamino acid. As a seed culture, the cells were pre-grown with 200 mL of the same medium in a 1 L baffled flask to an OD_{600} of ~28. The dissolved oxygen concentration of the fermentor was kept at 30% of air saturation by automatically increasing the agitation speed up to 800 rpm and then by changing the percentage of pure oxygen. A feeding solution (700 g L^{-1} glucose) was added into the fermentor using the pH-stat strategy when the pH rose to a value of greater than its set point (pH 7.0) by 0.05 due to the depletion of glucose. The culture pH was maintained at 7.0 by adding 1 M phosphoric acid or 28% (v/v) ammonia water. When the OD_{600} reached ~60, the cells were induced with 1 mM IPTG. Samples were periodically taken for the measurements of OD_{600} and preparation of protein samples as described for the flask cultivation.

2.3. Purification of secreted spidroins

The fermentation broth was centrifuged at 7,024*g* and 4 °C for 20 min, and the resulting supernatant was acidified with 1.32 M HCl to pH 4.0, and mildly agitated at room temperature for 2 h. After centrifugation at 15,422*g* for 10 min, the supernatant containing recombinant

MaSpI16 was precipitated by adding ammonium sulfate to 25% saturation, and incubated with magnetic agitation at room temperature for additional 1 h. In another setup for precipitation of the supernatant containing the larger spidroin MaSpI64, ammonium sulfate was added to 10% saturation. The mixtures were then centrifuged, and the resulting spidroin precipitates resolubilized in deionized water for various characterizations (described below). Alternatively, these protein solutions were concentrated to prepare spinning dopes using Amicon Ultra-0.5 Centrifugal Filter 10K devices (Millipore, Darmstadt, Germany) or lyophilized for storage.

2.4. SDS-PAGE analysis, protein quantification and characterization

For SDS-PAGE analyses, the protein samples were mixed with 5 × Laemmli sample buffer, boiled, centrifuged, and loaded onto 10% SDS-PAGE gels. Following electrophoresis, the gels were stained with Coomassie brilliant blue R250 (Generay, Shanghai, China) and scanned by the Bio-5000 plus scanner (Microtek, Shanghai, China). The protein bands were normalized and quantified by ImageJ software to estimate spidroin purity or secretory production level (% total extracellular proteins).

Protein concentration was routinely determined using the bicinchoninic acid (BCA) Protein Assay Kit from Pierce (Thermo Scientific, Rockford, IL). As the culture medium contained metal ions that interfered the BCA assay, the concentration of total proteins in the culture supernatant was estimated by using a Bradford Protein Quantification Kit (Yeasen, Shanghai, China). The extracellular spidroin titer was calculated by multiplying the concentration of total extracellular proteins and the spidroin secretory production level.

Protein secondary structures was studied by far-UV circular dichroism (CD) spectroscopy on a JASCO J-1500 spectropolarimeter (Tokyo, Japan). The CD spectra were collected from 190 to 260 nm at a resolution of 0.5 nm and a scanning rate of 100 nm min^{-1}. Each protein solution (0.2 mg mL^{-1}) was loaded into a 1 mm path length quartz cuvette, and equilibrated at 25 °C for 5 min before measurements. For each sample, three measurements were performed, and the averaged CD data were presented as mean residue ellipticity ([θ], deg cm^2 $dmol^{-1}$).

The size distribution profile of purified silk protein in solution was studied by dynamic light scattering (DLS) on a Zetasizer Nano ZS instrument (Malvern Instruments Ltd., Worcestershire, UK). The water solution of each purified spidroin (5 mg mL^{-1}) was introduced into the cuvettes and equilibrated at 25 °C for 1 min prior to measurements. For each sample, three measurements were performed and averaged.

2.5. Protein immunoblotting

Protein extracts from the *C. glutamicum* cells, culture supernatants, and purified silk proteins were analyzed by immunoblotting with anti-polyhistidine antibody to detect the recombinant spidroins expressed. Briefly, the protein samples were resolved on the SDS-PAGE gels described above, and transferred to PVDF membranes using Wet type blotting device (Bio-Rad). After blocking with 5% (w/v) nonfat milk in the TBST buffer (10 mM Tris-HCl, pH 8.0, 150 mM NaCl, 0.05% Tween 20), the membranes were incubated with 2,000-fold diluted monoclonal anti-polyhistidine-peroxidase conjugate (Sigma product no. A7058) at room temperature for 2 h. Immunoreactive bands were detected using an enhanced chemiluminescence reagent (BeyoECL Moon; Beyotime, Shanghai, China).

2.6. Fiber spinning and characterization

For fiber spinning, a tailor-made microfluidic spinning apparatus reported by Hu et al. (2021) was used, which possessed a progressively narrowing fluidic channel to mimic the shape of spider's major ampullate gland. More specifically, the width of the channel decreased from an initial 2590 μm to the terminal 100 μm. Dope solutions with a protein concentration of 40% (unless otherwise specified) were injected into the microfluidic channel using a pump at a speed of 5 μL min^{-1}, and further extruded into a coagulation bath containing 90% ethanol at room temperature. The length of the as-spun fibers could reach ~20 m. The as-spun fibers were subsequently cut into 20 mm lengths and transferred into an 80% ethanol bath for 2 h. For fiber stretching, one end of each fiber was fixed and the other end was continuously stretched to 4 times its original length at a speed of 1 mm s^{-1}. These fibers were kept in the 80% ethanol bath for additional 1 h. The drawn fibers were then removed from the bath and dried at room temperature under tension to prevent fiber contraction.

For characterization of the surface and cross-section of the post-drawn fibers, a Hitachi S–3400N scanning electron microscope (Tokyo, Japan) was used. Prior to the analyses, the fibers were frozen and fractured in liquid nitrogen to obtain fracture cross-sections. The fibers were then coated with gold using a Leica EM SCD050 sputtering device equipped with a water-cooled sputter head (Leica Microsystems GmbH, Vienna, Austria). The ImageJ software version 1.8.0_112 was used to determine the cross-sectional area (CSA) of the fiber specimens.

For mechanical testing, the post-drawn fibers were loaded onto an Instron 5944 testing machine with a 10 N load cell (Instron Corporation, Norwood, MA), and tested at 20 °C and 60% relative humidity. The gauge length of each fiber tested was 1 cm, and the stretching rate was set at 4 mm min^{-1}. The engineering strain was defined as the ratio of change in length and the original length, and the engineering stress was obtained as the ratio of force and the original CSA of the fiber. Mechanical data derived from the engineering stress-strain curves are shown as means ± standard deviation ($n = 10$).

To characterize molecular alignment in the synthetic fibers, polarized Raman spectromicroscopy was performed with an inVia Qontor confocal Raman spectrometer (Renishaw, Gloucestershire, UK) coupled to a Leica microscope (DM 2700M). A polarizer was placed before the entrance slit of the monochromator to allow the detection of the polarized scattered light along the X and Y directions. The fibers were gently mounted on glass microscope slides with double-sided tape, and initially aligned toward the X-axis. The fibers were first irradiated at a fixed point with a 785 nm edge laser with polarization fixed along the X-axis and focused through a 50 × objective (with a numerical aperture NA = 0.5). The polarized Raman spectra were subsequently acquired from 784 cm^{-1} to 1866 cm^{-1} with a 1200 lines/mm grating, and recorded as I_X. For each acquisition, a total of 8 spectra were accumulated, each for 8 s. The fibers were then rotated along the Y-axis with the same laser polarization to obtain the Raman spectra as I_Y. All measured spectra were analyzed using the WiRE 5.1 software from Renishaw and normalized to the intensity of the 1450 cm^{-1} peak, which arises from CH_2 bending and is insensitive to protein conformation. As a qualitative marker of the level of orientation, I_Y/I_X was calculated using the normalized peak intensity at 1669 cm^{-1}, and the calculated intensity ratio was averaged from three replicates for each type of the synthetic fibers.

3. Results

3.1. Sec-dependent secretion of recombinant spidroins and screening of signal peptides

So far, there has been no report on the secretory production of recombinant spidroins in Gram-positive bacteria. We thus aimed at establishing such secretory platform in the industrially robust Gram-positive bacterium *C. glutamicum*. It is known that *C. glutamicum* has two major secretory pathways, the general secretory (Sec) pathway and the twin-arginine translocator (Tat) pathway, both of which have specific signal peptides that mediate the export of target proteins into the culture medium (Watanabe et al., 2009). For the secretory production of spider silk protein, we first assembled a codon-optimized synthetic gene encoding 16 repeats of the consensus sequence of spider *T. clavipes*

MaSpI. The encoded protein (hereafter referred to as MaSpI16) was fused N-terminally to a hexahistidine tag and C-terminally to a Sec- or Tat-dependent signal peptide. Recombinant plasmids for the expression of these fusion genes under the IPTG-inducible *tac* promoter (Fig. 1A) were constructed based on the *E. coli-C. glutamicum* shuttle vector pXMJ19.

Expression and secretion studies were conducted using *C. glutamicum* RES167 as the host strain, which is a restriction-deficient derivative of the wild-type ATCC 13032 strain. After flask cultivation of the recombinant strains in the rich BHI medium, the protein fractions of the culture supernatants and cell lysates were analyzed by SDS-PAGE and Western blot as described in the Method section. As shown in Fig. 1B, the Cg1514 signal peptide, which was recently identified from *C. glutamicum* and proven to be Sec-dependent (Yim et al., 2016), was capable of mediating secretory production of the 16-mer silk protein MaSpI16. In addition, this model recombinant spidroin was produced as a major protein in the culture medium with a high purity (~78% of total proteins in the culture supernatant). Two previously known Tat-dependent signal peptides, Cg0955 signal peptide (Teramoto et al., 2011) and *E. coli* TorA signal peptide (Kikuchi et al., 2009), were also tested. Although they successfully mediated export of green fluorescent protein, a folded cargo known to specifically secrete through the Tat pathway (Teramoto et al., 2011; Yim et al., 2016), neither of them enabled secretory production of MaSpI16 (Fig. S1). These results indicated that the repetitive recombinant spidroin can be secreted via the Sec-dependent pathway, but less likely via the Tat-dependent pathway in *C. glutamicum*.

It was reasoned that the spidroin secretion level might be increased by recruiting more suitable Sec-dependent signal peptides (Freudl, 2018). Thus, a library of Sec-dependent signal peptides that have previously been shown to mediate efficient secretory production of enzymes (Watanabe et al., 2009; An et al., 2013) was examined. Indeed, 5 of the 16 signal peptides screened resulted in markedly increased amounts of secreted silk protein when compared to the Cg1514 signal peptide tested first (Fig. 1C). In particular, the signal peptide of Cg2196 (a putative secreted or membrane protein) allowed approximately twofold higher secretion of the 16-mer silk protein. In contrast, the signal peptides of Cg0316 and Cg2402 were incapable for secretory production of the silk protein even though these two peptides were previously ranked medium to high in efficiency for the secretion of α-amylase (Watanabe et al., 2009). These results clearly suggested the importance of screening a library of signal peptides for the improved export of a specific protein of interest, and in particular the silk protein as this class of repetitive proteins has not previously been targeted for secretion in *C. glutamicum*. Furthermore, the identity of the secreted 16-mer silk protein and correct cleavage of the Cg2196 signal peptide during Sec-dependent export were verified by MALDI-TOF mass spectrometry and N-terminal amino acid sequencing (Fig. S2). Therefore, the Cg2196 signal peptide was used in subsequent studies.

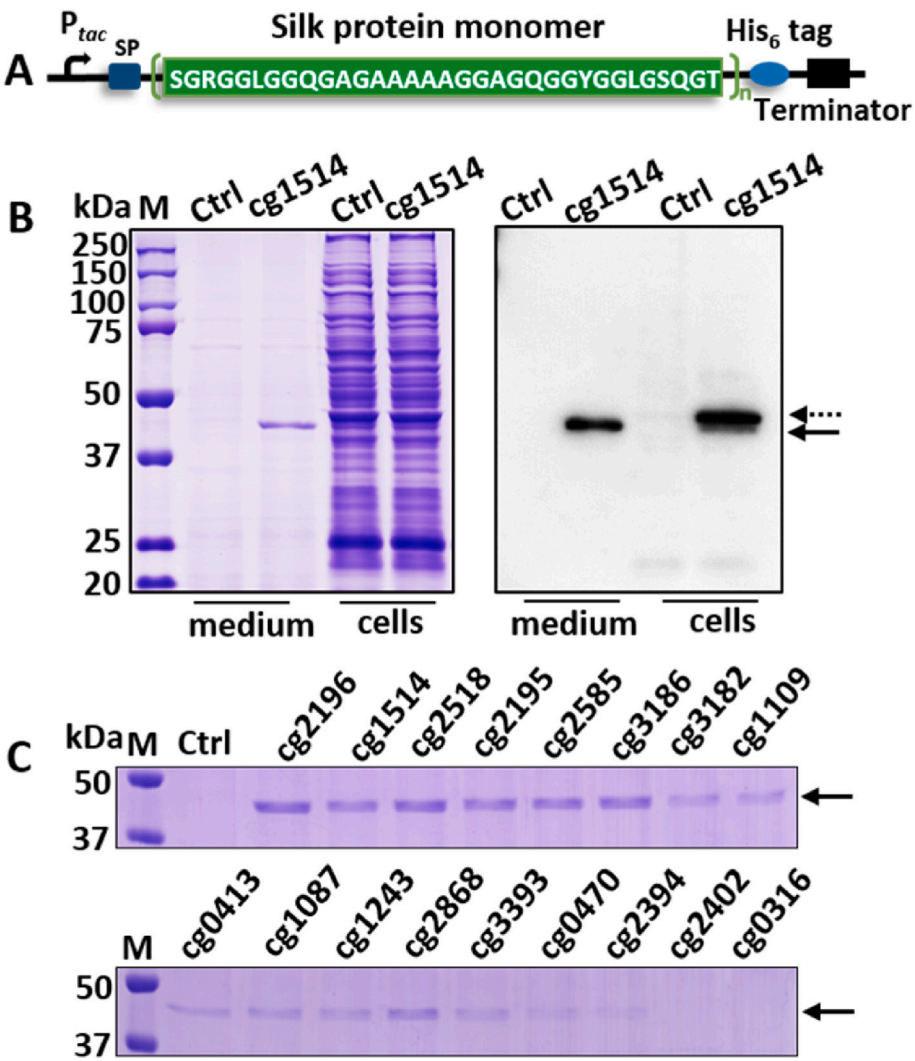

Fig. 1. Sec-dependent export of recombinant spidroins. (**A**) Schematic diagram of genetic constructs for secretory production of recombinant spidroins. (**B**) Coomassie-stained SDS–PAGE gel (*Left*) and Western blot (*Right*) analysis of culture supernatants and lysates of *C. glutamicum* RES167 cells carrying empty vector (Ctrl) and plasmid for secretory production of the His6-tagged 16-mer spidroin by C-terminal fusion to the Sec-dependent cg1514 signal peptide. The arrow indicates the target protein in the medium, and the dotted arrow indicates the cytoplasmic preprotein with intact signal peptide. (**C**) SDS–PAGE analysis of culture supernatants reveals signal peptides (indicated above each lane) suitable for high-level secretory production of the 16-mer spidroin.

3.2. Engineering of the host strain to improve secretory production

Next, the *C. glutamicum* chassis strain was engineered for further increasing the secretory production level. To this end, we attempted to improve extracellular spidroin titers at the gene dosage/transcription, translation, and secretion levels (Fig. 2A). Accordingly, the preceding *C. glutamicum* strain RES167 was genetically engineered, and the derivative strains were then tested for secretion of the 16-mer MaSpI16 and its higher molecular weight version MaSpI64 having 64 repetitive consensus sequence (theoretical molecular weight of 168.92 kDa).

Due to the highly repetitive nature of the spidroin genes, improving the genetic stability of the recombinant plasmids via attenuation of host recombination activities was thought to be important; this would give the effect similar to increasing the gene dosage. Thus, the *recA* gene encoding the main recombinase was knocked out from the *C. glutamicum* chromosome. As expected, the *recA* mutant (*C. glutamicum* JQ01) improved secretion of both MaSpI16 (13% higher) and MaSpI64 (27% higher) compared to the control strain (Fig. 2B; Fig. S3). Surprisingly, analyses of the plasmid copy numbers revealed that the spidroin gene dosage was similar in the strains with and without *recA* disruption (Fig. S4A). On the other hand, the silk gene transcript level was drastically elevated in the *recA* mutant (Fig. S4B), which is expected to result in improved spidroin biosynthesis for export into the culture medium. Although the underlying molecular events and mechanisms remain to be studied, these results suggest a previously unknown target (*recA* disruption) for improving secretory production of repetitive proteins at

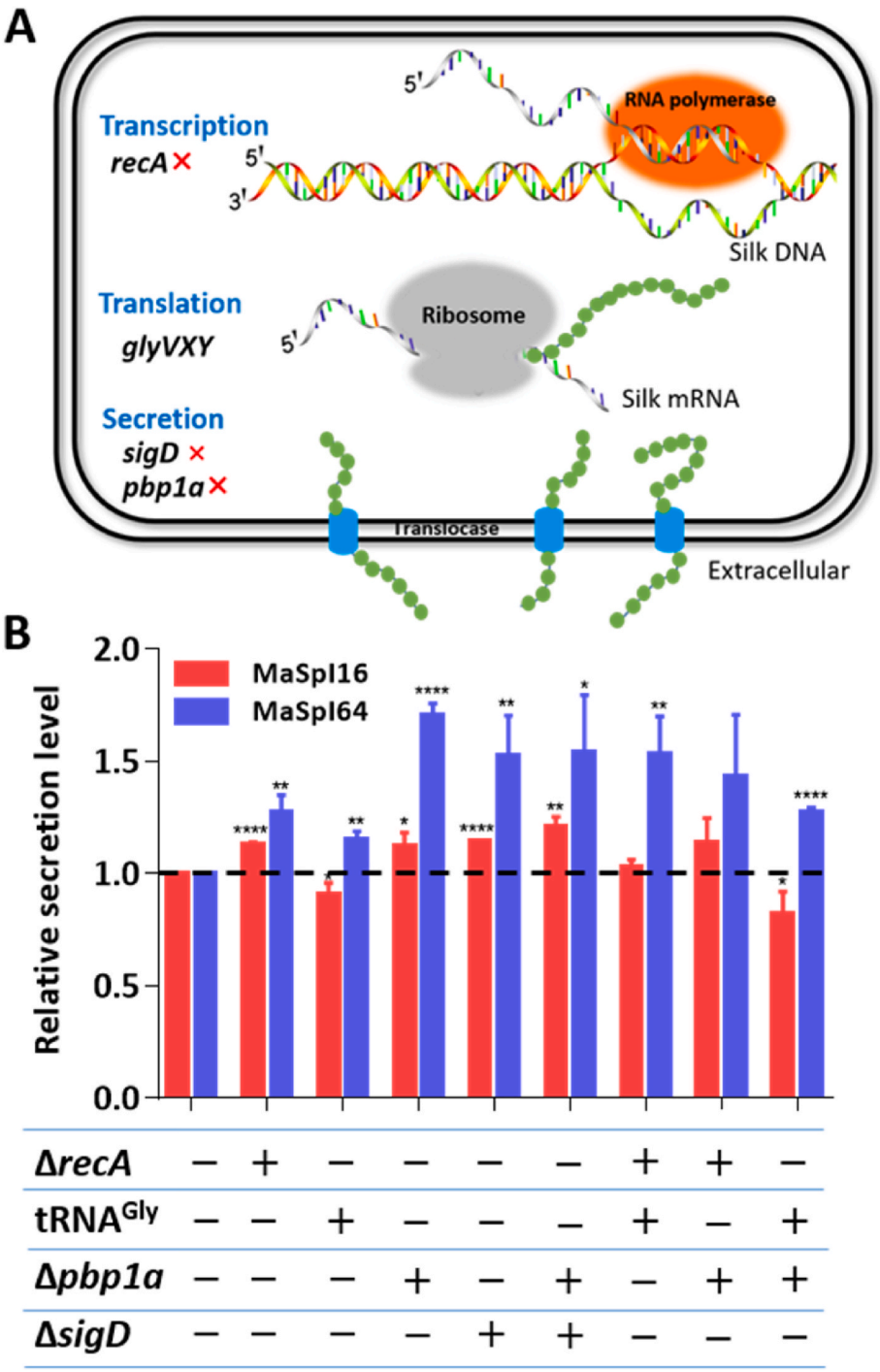

Fig. 2. Engineering of the *C. glutamicum* chassis strain for improving the secretory production level. (**A**) Schematic diagram of engineering at spidroin gene transcription, translation and secretion levels. The gene targets include *recA*, *glyVXY*, *pbp1a*, and *sigD* encoding recombinase A, tRNAs that recognize glycine codons GGU and GGC, membrane carboxypeptidase, and RNA polymerase sigma factor SigD, respectively. (**B**) Relative secretion levels of MaSpI16 and MaSpI64 in each engineered strain compared to the non-engineered RES167 strain. Data are presented as mean ± s.d. of $n = 3$ biologically independent samples. Statistical significance was determined using one-way ANOVA (*$P < 0.05$; **$P < 0.01$; ****$P < 0.0001$).

the transcription level.

As spidroins are particularly rich in glycine and alanine, spiders produce unusually large tRNA pools for these amino acids to meet the increased demand during silk protein synthesis (Candelas et al., 1990). This has inspired our and other groups to improve recombinant spidroin production at the translational level in *E. coli* by engineering the relavant amino acid biosynthetic pathway and aminoacyl-tRNA synthetase (Xia et al., 2010; Cao et al., 2017). Thus, the *glyVXY* gene cassette encoding the tRNAs that recognize the dominant glycine codons was overexpressed. It was found that the overexpression of $tRNA^{Gly}$ increased the secretion level of MaSpI64 by 15%, but unexpectedly, slightly reduced the secretion level of MaSpI16 (Fig. 2B). It seems that elevating the $tRNA^{Gly}$ pool was benificial for the increased production and secretion of the higher molecular weight MaSpI64 requiring more $tRNA^{Gly}$, whereas $tRNA^{Gly}$ availability might not be limiting in translating the smaller spidroin MaSpI16.

Then we attempted to increase spidroin export by improving the cell wall permeability. There are two permeability barriers for protein export in *C. glutamicum*, the inner peptidoglycan layer and the outer mycolic acid layer (Houssin et al., 2020). It has been reported that penicillin-binding-proteins such as PBP1a are crucial for peptidoglycan synthesis in *C. glutamicum*, and have function related to protein secretion (Matsuda et al., 2014). In addition, sigma factor SigD is involved in modifying peptidoglycan cross-linking and improving mycolate synthesis. In order to attenuate the two cell wall permeability barriers, the *pbp1a* and *sigD* genes were knocked out from the chromosome of *C. glutamicum* RES167, and the two single mutants (JQ02 and JQ03) were then tested for secretory spidroin production. As shown in Fig. 2B, both mutants showed improved secretory production, and the positive effect was more pronounced for the larger spidroin MaSpI64. Notably, MaSpI64 secretion level was ~70% higher in the Δ*pbp1a* mutant than the control strain RES167. To see if the beneficial effects of disrupting *pbp1a* and *sigD* genes are synergistic, the Δ*pbp1a* Δ*sigD* double mutant (JQ04) was constructed as well. However, this double mutant strain did not further increase spidroin secretion. In addition, when compared to the Δ*pbp1a* mutant, the double mutant and the Δ*sigD* mutant released more endogenous proteins into the culture medium (data not shown), which is undesirable as this would complicate the downstream spidroin purification. Thus, *pbp1a* disruption was employed as the strategy for the increased spidroin secretion.

With the identified gene targets at the transcription (Δ*recA*), translation (*glyVXY* overexpression) and secretion (Δ*pbp1a*) levels, the effects of combining the individual engineering strategies were examined next. All these combinations resulted in higher spidroin secretion levels than the control RES167 strain. However, none of these combinations was superior to the *pbp1a* single knockout strain, which was demonstrated to be the best strain. It appeared that *pbp1a* knockout masked the beneficial effects of engineering at the transcription and translation levels, indicating that the silk protein export pathway was the major barrier in the secretory production.

3.3. High cell density cultivation in bioreactors

In order to further increase the secretory production levels, high cell density fed-batch culture of the above engineered strains were perfomed in a semi-defined medium using a 5 L jar fermentor (see Methods). Here the recombinant Δ*pbp1a* cells harboring plasmids pCG8-I16cg and pCG8-I64cg were shown as typical examples for high-level extracellular production of MaSpI16 and MaSpI64, respectively. As shown in Fig. 3 (*upper panels*), the two recombinant strains could be grown to a high OD_{600} of ~290, using a pH-stat strategy for glucose feeding. Under the same cultivation conditions, the recombinant RES167 strains having the intact *pbp1a* could be grown to comparable biomass concentrations (Fig. S5). These results verified that attenuation of the inner

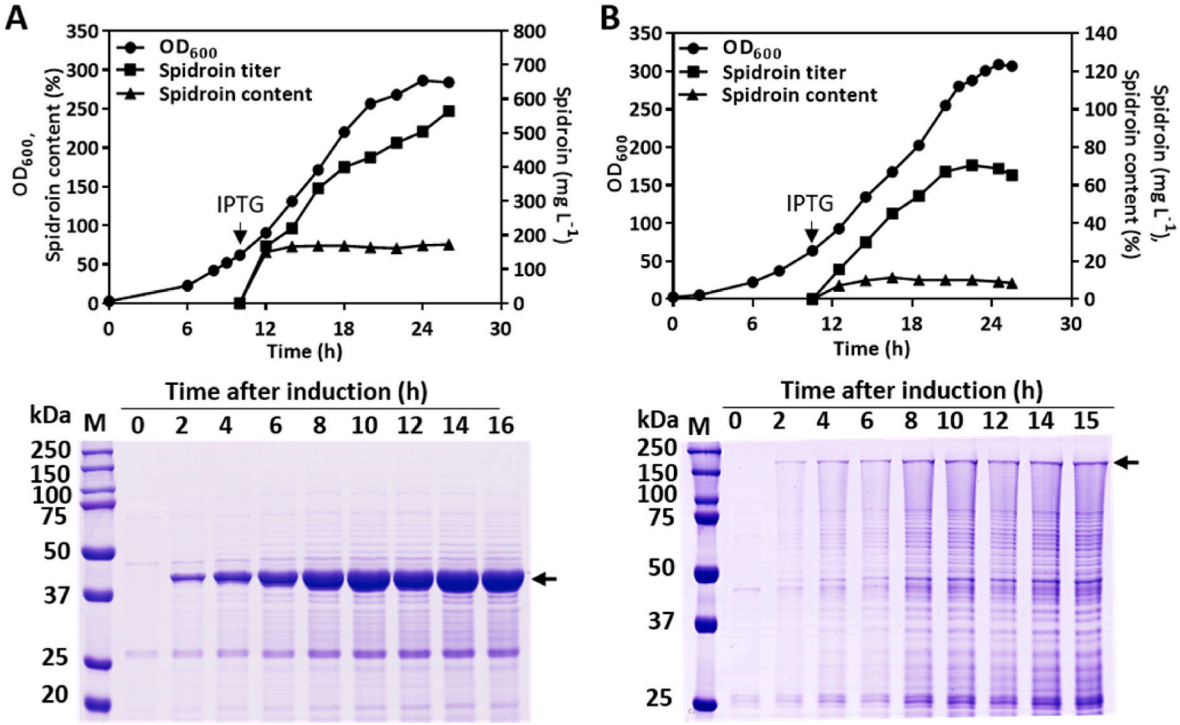

Fig. 3. Secretory production of recombinant spidroins by high cell density cultivation. The recombinant Δ*pbp1a* strains harboring pCG8-I16cg (**A**) and pCG8-I64cg (**B**) were cultivated in a semi-defined medium using a 5 L fermentor. The time profiles of biomass (OD_{600}), spidroin content (% of total extracellular proteins), and extracellular spidroin titer are shown (*Upper panels*). When the cell OD_{600} reached ~60, the cells were induced with 1 mM IPTG at the indicated time. Following induction, extracellular protein samples of the culture supernatants were analyzed on SDS-PAGE gels (*Lower panels*). Loaded on the gels were aliquots corresponding to 2 μL of culture medium for spidroin MaSpI16 and 4 μL of culture medium for MaSpI64, and the arrows indicate the respective target spidroins. Data in **A** and **B** are representative of $n = 2$ independent experiments.

peptidoglycan layer by *pbp1a* disruption did not adversely affect the capability of the *C. glutamicum* cells to grow to a high cell density, indicating its good application potentials in even larger scale fermentation.

The titer of secreted MaSpI16 in the culture supernatant increased steadily to a high level of 554.7 ± 13.2 mg L^{-1} (Fig. 3A). In addition, the content of MaSpI16 (% of total extracellular proteins based on SDS-PAGE analysis) increased drastically within 2 h IPTG induction to a high level of 65.8%, and plateaued thereafter until the end of fed-batch cultivation (75.6%). This fascinating result suggested that the secreted spidroin was abundant and predominant in the cell-free culture medium, representing two features that are highly desirable for facile recovery of the spidroin. On the other hand, the content of MaSpI64 increased to the maximal value of ~11.3% at 6 h post-induction, and the extracellular titer of MaSpI64 reached its maximal level of 68.0 ± 3.7 mg L^{-1} at 12 h post-induction. It appeared that the recombinant cells did not secrete more MaSpI64 into the culture medium in the late stage of fed-batch fermentation, and instead released more endogenous proteins, as could be seen by the SDS-PAGE analysis (Fig. 3B). The titer of secreted MaSpI64 was thus decreased slightly at the end of fermentation as a result of dilution due to addition of the feeding solution into the fermentor.

In side-by-side comparison (*lower panels* of Fig. 3), much more high molecular weight proteins (below silk protein) were observed in the secretory production of MaSpI64 than those in the production of MaSpI16. To explore whether these proteins are derivatives of MaSpI64, the protein bands at ~120 and 50 kDa were excised from the SDS-PAGE gel, digested with trypsin, and identified by LC-MS/MS (Fig. S6). The peptide sequencing revealed the existence of truncated versions of the silk protein MaSpI64 in the culture supernatant (Fig. S6A). We further examined whether this was due to degradation of the MaSpI64 protein by extracellular protease(s) by incubating the culture supernatant at 30 °C with and without protease inhibitors. The results proved that the truncation was unlikely due to extracellular proteolysis (Fig. S6B). It was possible that the extracellular, lower molecular weight versions of MaSpI64 were due to secretion of the truncated silk protein species resulting from cytosolic synthesis truncation, which has been reported to occur in heterologous production hosts and even in spiders (Candelas et al., 1983; Bhattacharyya et al., 2021; Fahnestock and Bedzyk, 1997).

3.4. Purification of secreted spidroins and preparation of concentrated aqueous dopes

Next we developed an integrated process for spidroin purification and preparation of concentrated spidroin solutions that can be directly utilized as dopes for fiber spinning (Fig. 4A). Initially we focused on MaSpI16 purification because of its abundance and predominance in the culture medium. After clarification of the fermentation broth via centrifugation, the cell-free supernatant was acid precipitated to remove host cell proteins that were also secreted by the *C. glutamicum* chassis

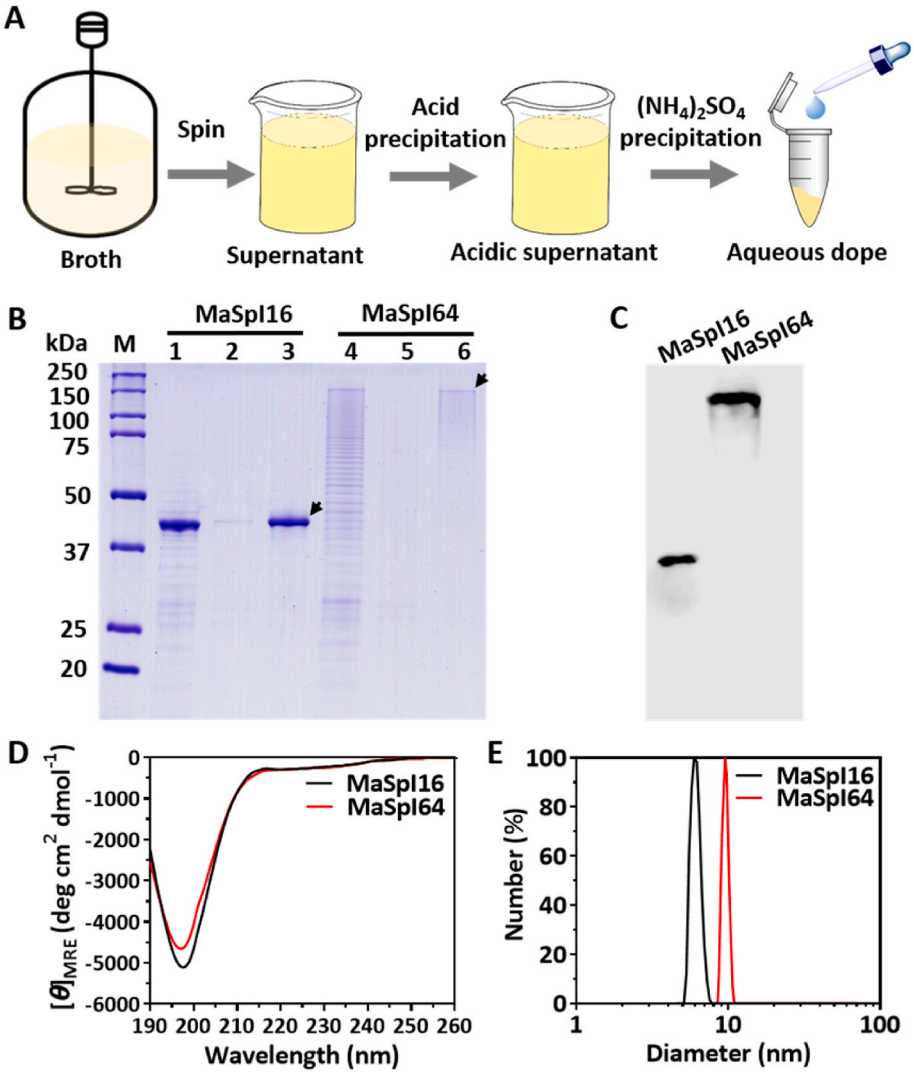

Fig. 4. Chromatography-free purification and characterization of the secreted spidroins. (**A**) Schematic diagram of collecting cell-free supernatant from the fed-batch broth, acid precipitation, ammonia sulfate precipitation, resolubilization, and concentration to prepare purified spidroin dopes. (**B**) SDS-PAGE analysis of the protein samples in the purification procedure shown in **A**. Lanes 1 and 4, cell-free supernatants; Lanes 2 and 5, pellets from supernatants with acidification at pH 4.0; Lanes 3 and 6, precipitates after $(NH_4)_2SO_4$ treatment. The arrows indicate the target spidroins on the gels. (**C**) Western blot analysis of the purified spidroins using monoclonal anti-polyhistidine-peroxidase conjugate. (**D**) Far-UV CD spectra and (**E**) dynamic light scattering (DLS) size distribution profiles of the purified spidroins.

during the fed-batch fermentation (Fig. 4B, lanes 1 and 2); this operation is based on the observation that recombinant spider dragline proteins composed of repetitive consensus sequences are soluble under acidic condition because they are highly positively charged (Xia et al., 2010). The target silk protein was then enriched by ammonium sulfate precipitation, and resolubilized with deionized water. The resulting aqueous solution of MaSpI16 had a protein concentration of ~100 mg mL^{-1}, a purity of approximately 93.0%, and a recovery yield of 84.9%, as revealed by the SDS-PAGE analysis (Fig. 4B, lane 3). This facile chromatography-free purification approach was also used to purify MaSpI64 from the culture medium. A comparable protein recovery yield (89.1%) was obtained for the larger spidroin; however, the purity of MaSpI64 was inferior (47.1%), which might be due to less efficient staining of the large molecular weight spidroin compared to the contaminant host proteins (see discussion below). The N-terminal sequence of the purified MaSpI64 was determined by chymotrypsin digestion and tandem mass spectrometric analysis, which verified correct cleavage of the signal peptide in secretion (Fig. S7). Furthermore, the two purified spidroins were confirmed by Western blot using a monoclonal anti-polyhistidine-peroxidase conjugate (Fig. 4C).

Next, the secondary structure and aggregation state of the purified spidroins were analyzed. Far-UV CD spectroscopy revealed that the two spidroins showed a typical random coil structure (Fig. 4D), indicative of their disordered feature in aqueous solution. In addition, the monodispersity and aggregation state of the purified spidroins in solution were monitored by dynamic light scattering measurements of hydrodynamic radius. The recombinant spidroins were homogenous in size in the aqueous solutions, and existed mainly as single protein chains without the presence of protein aggregates (Fig. 4E).

It is well recognized that spider dragline silk dopes are highly concentrated, with a protein concentration estimated to be 25−30% (w/v) by dope drying (Chen et al., 2002; Holland et al., 2006) and ~50% by solution NMR of ^{13}C labeled dope (Hijirida et al., 1996). To test solubility of the recombinant spidroins secreted by *C. glutamicum*, the aforementioned water solution of purified MaSpI16 were concentrated by centrifugal ultrafiltration. Surprisingly, the solubility of MaSpI16 reached a remarkable protein concentration of 66% (w/v), which exceeded the aqueous solubility of native dragline silk dopes and their recombinant counterparts reported in previous studies (Andersson et al., 2017; Hu et al., 2021). In addition, the water solution of purified MaSpI64 could be concentrated to a high protein concentration in the range of 40–47% (w/v). Taken together, these results demonstrated successful recapitulation of high aqueous solubility in the secreted spidroins, and consolidated preparation of highly concentrated dopes without the commonly used organic solvents such as hexafluoroisopropanol and formic acid (Bowen et al., 2018; Copeland et al., 2015; Foong et al., 2020; Jones et al., 2015; Xia et al., 2010).

3.5. Synthetic fiber spinning and characterization

With the above silk protein dopes in hand, spinning of these dopes into synthetic fibers was performed. As the conditions under which the synthetic fibers were spun and processed are critical in determining the fiber mechanical properties (Lazaris et al., 2002), wet spinning of the fibers was performed under essentially the same conditions (e.g., the spinning apparatus, spinning solution injection speed, coagulation bath, and post-spinning drawing process). To explore the relation between the size of the secreted spidroin, spinning dope concentration, and the mechanical properties of spun fibers, three dopes (40% MaSpI16, 40% MaSpI64, and 60% MaSpI16, all in w/v) were tested for fiber spinning. Each dope was pumped into a coagulation bath (90% v/v ethanol) using a tailor-made microfluidic apparatus as reported in our recent study (Hu et al., 2021), which possessed a progressively narrowing fluidic channel that mimics the shape of spider's major ampullate gland. The resulting continuous fibers were collected and processed by drawing to 4 times of their original length. These post-drawn fibers were extensively characterized in terms of mechanical, morphological and microstructural properties (see results below). For clarity, the fibers derived from the 40% MaSpI16, 40% MaSpI64, and 60% MaSpI16 dopes were termed MaSpI16, MaSpI64, and MaSpI16 HD fibers, respectively.

The mechanical properties of the above three types of synthetic fibers were examined by tensile tests under identical conditions. The representative engineering stress−strain curves of these fibers are shown in Fig. 5A. These curves reveal several important mechanical properties of the fiber such as the ultimate tensile strength, breaking strain (extensibility), Young's modulus (the slope of a curve as a measure of the fiber's stiffness), and toughness (the area under the stress−strain curve as a measure of the fiber's ability to absorb energy before rupture). The overall mechanical properties of the synthetic fibers markedly increased with an increase in the silk protein size or the protein concentration in spinning dope, except that the fiber's stiffness was unaffected (Fig. 5B–E). For example, the MaSpI64 fibers exhibited a breaking strain of 59.3 ± 11.1%, which was ~3.7-fold higher than that of the MaSpI16 fiber (16.2 ± 6.7%). Of particular interest, the 60% dope-derived MaSpI16 HD fibers exhibited a breaking strain of 51.5 ± 19.5%, strength of 168.8 ± 32.5 MPa, and toughness of 70.0 ± 30.3 MJ m^{-3}. Such mechanical properties are essentially comparable to the values of the higher molecular weight MaSpI64 fibers. In view of the secretory production titer (Fig. 3), purity (Fig. 4B) and solubility, fabrication of the MaSpI16 HD fibers is more efficient than the MaSpI64 fibers. Notably, the toughness of the MaSpI16 HD fibers reached 63% of the value for the native dragline silk (111.19 ± 30.54 MJ m^{-3}; Swanson et al., 2006), which is appreciable and may be further improved by optimizing the spinning and posttreatment conditions.

Next, we examined the morphological features of the synthetic fibers by scanning electron microscopy (SEM). Analysis of fiber surface revealed that all the three types of synthetic fibers had fibrillar structure, among which the MaSpI16 HD fiber was smoothest and most compact (Fig. 6A). Cross section analysis revealed that the MaSpI16 and MaSpI64 fibers had irregular or strongly elliptical cross sections (Fig. 6B), which are not uncommon in synthetic dragline silk fibers (Bowen et al., 2018; Weatherbee-Martin et al., 2016; Saric et al., 2021) and even natural dragline silks (Blackledge et al., 2005). In contrast, the MaSpI16 HD fiber had fairly circular cross section, with microfilaments densely compacted along the fiber axis.

The structural features of the synthetic fibers were further examined at the molecular level by Fourier transform infrared spectroscopy (FTIR) and polarized Raman spectromicroscopy. According to a previously reported protocol (Hu et al., 2006), deconvolution of the amide I regions of the FTIR spectra was performed to estimate the contents of fiber secondary structures such as crystalline β-sheet, random coil/α-helix, β-turn and weak β-sheet (Fig. S8). It was found that the contents of crystalline β-sheet were 28.36 ± 1.33% and 27.34 ± 1.99% for the MaSpI16 and MaSpI64 fibers, respectively, whereas the MaSpI16 HD fiber had a significantly higher level at 32.12 ± 1.46%. This number is comparable to that of spider *T. clavipes* dragline silk (34%) which is believed to be the key element in the natural silk responsible for the high tensile strength (Jenkins et al., 2010). Finally, we investigated the β-sheet alignment along the fiber axis as this is also an important structural feature of natural dragline silk that contributes to the exceptional mechanical properties (Yarger et al., 2018). Therefore, the orientational parameter $I_{Y/X}$ was estimated to obtain semiquantitative characterization of the level of molecular orientation (Rousseau et al., 2009). To this end, we compared the amide I β-sheet component (1669 cm^{-1}) peak intensities between Raman spectra acquired from the fibers oriented both parallel (X-axis) and perpendicular (Y-axis) to the direction of laser polarization (Fig. S9). The $I_{Y/X}$ values of the MaSpI16, MaSpI64 and MaSpI16 HD fibers were 0.98 ± 0.06, 1.29 ± 0.14 and 1.14 ± 0.08, respectively (Fig. 6C). This was indicative of substantial β-sheet anisotropy in the MaSpI64 and MaSpI16 HD fibers, in contrast with the MaSpI16 fiber with poor axial β-sheet crystal alignment. Taken together, the above results suggested that both the crystalline β-sheet fraction and

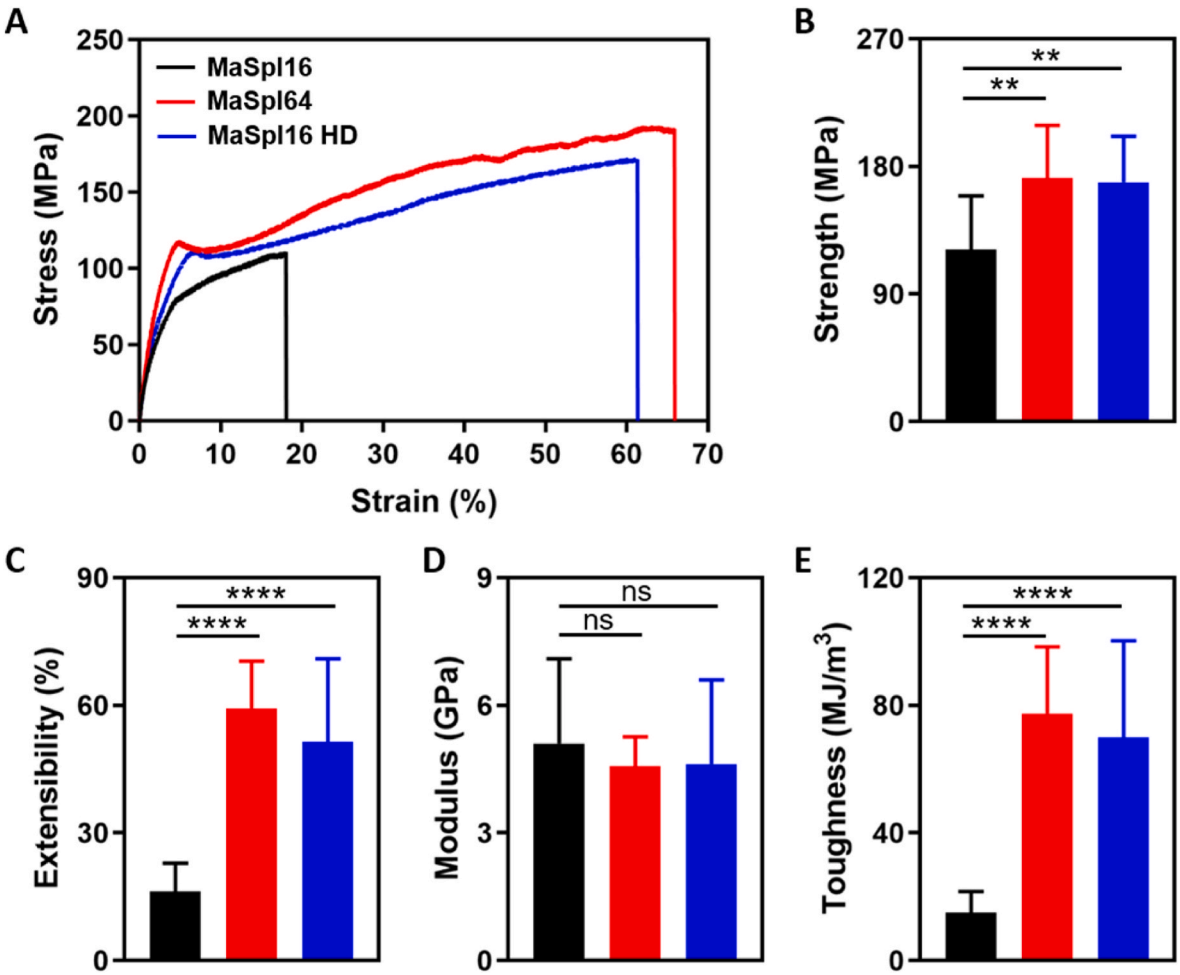

Fig. 5. Tensile mechanical properties of the fibers. (**A**) Representative engineering stress−strain curves, (**B**) strength, (**C**) extensibility, (**D**) Young's modulus, and (**E**) toughness from tensile testing of the fibers. Data in **B**−**E** are presented as mean ± s.d. of $n = 10$ independent fiber samples derived from 40% MaSpI16 (black bars), 40% MaSpI64 (red bars) and 60% MaSpI16 (blue bars) protein solutions. Statistical significance was determined using one-way ANOVA (ns, not significant with $P > 0.05$; $^{**}P < 0.01$; $^{****}P < 0.0001$). (For interpretation of the references to color in this figure legend, the reader is referred to the Web version of this article.)

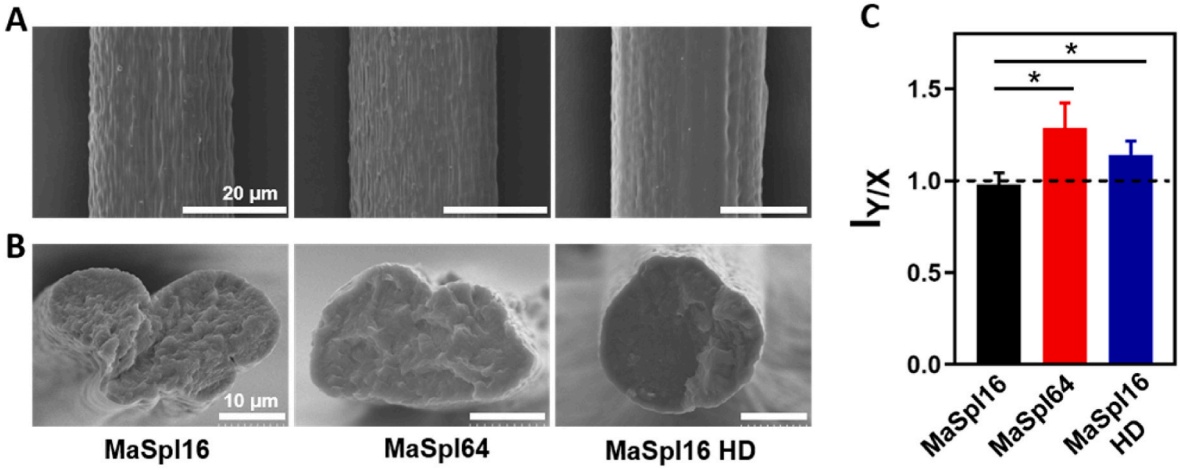

Fig. 6. Morphological and structural characterization of the synthetic fibers. Scanning electron microscopy analyses of (**A**) fiber surfaces and (**B**) cross-sections. (**C**) The orientational parameter $I_{Y/X}$ of the fibers. Data are presented as mean ± s.d. of $n = 3$ independent fiber samples derived from 40% MaSpI16, 40% MaSpI64 and 60% MaSpI16 solutions, respectively. Statistical significance was determined using one-way ANOVA ($^{*}P < 0.05$).

alignment contribute to the superior strength and toughness values found for the MaSpI64 and MaSpI16 HD fibers.

4. Discussion

In this study, we reported the development of engineered *C. glutamicum* platform strains capable of high-level secretory production of recombinant spider dragline silk proteins. This goal was achieved by the following strategies: (1) assembly of synthetic spider dragline silk genes, (2) identification of the general Sec-dependent secretory pathway for the export of disordered silk proteins, (3) screening of robust translocation signal peptides, (4) multiplexed engineering of the host strain for improving silk gene transcription, translation, and protein translocation, and (5) intensification of the secretory production capacity by HCDC.

As a Gram-positive bacterium, *C. glutamicum* has long been considered to excrete only a limited number of endogenous proteins into the extracellular medium. According to Hermann et al. (2001), *C. glutamicum* wild-type ATCC 13032 secreted ~18.5 mg L^{-1} of endogenous proteins when the strain was grown in a minimal medium in flask cultivation to an OD_{600} of ~17, and exhibited a secretion capacity of ~1.1 mg L^{-1} OD_{600}^{-1} by normalizing the biomass. Those secreted proteins were further analyzed by two-dimensional gel electrophoresis leading to the observation of about 40 protein spots. Another study on extracellular proteome of the wild-type *C. glutamicum* ATCC 13032 revealed a total of 99 spots corresponding to 54 different proteins (Hansmeier et al., 2006). In line with these previous results, we observed around 30 protein bands on the SDS-PAGE gel of the culture supernatants from the HCDC of recombinant RES167 harboring empty vector pCG8 (Fig. S5C). This recombinant strain, which was a restriction deficient mutant of the wild-type ATCC 13032, showed a protein secretion capacity of 2.0-2.6 mg L^{-1} OD_{600}^{-1} during the fed-batch cultivation. It is striking to note that the amount of proteins secreted from the HCDC of *C. glutamicum* exceeded 0.6 g L^{-1} at the end of fermentation (Fig. S5C), which was much higher than that expected from previous flask culture studies. This observation once again indicated the good potential of *C. glutamicum* for protein secretion, and inspired us to engineer it into a secretory producer.

The *C. glutamicum* secretory platform developed in this study enabled extracellular production of the recombinant spidroins at titers that are sufficiently high for downstream purification and synthetic fiber spinning. For example, the highest secretion titers for MaSpI16 (43.36 kDa) and MaSpI64 (168.92 kDa) were 554.7 ± 13.2 mg L^{-1} and 68.0 ± 3.7 mg L^{-1}, respectively (Fig. 3). It should be noted that the secretion titer sharply decreased as the size of the target silk protein increased. This protein molecular weight-dependent secretion is not surprising, which might be due to the difficulties in *de novo* biosynthesis and export of the larger recombinant spidroin in the bacterial expression host. Indeed, previous studies have shown that the highly repetitive nature of the silk gene constructs, high GC content (~70%) of the genes, and the glycine-rich (>40%) feature of the silk proteins, make the spidroin extremely difficult to express even in the favorate model bacterium *E. coli* (Xia et al., 2010; Yang et al., 2016). Furthermore, as shown in Fig. 4E, the hydrodynamic diameter of MaSpI64 in solution (~10 nm) was larger than that of MaSpI16 (~6 nm), which likely makes the higher molecular weight spidroin more difficult to translocate through the Sec-dependent secretion channel of *C. glutamicum*.

The above spidroin secretion titers were estimated by multiplying the concentrations of total proteins in the cell-free culture supernatants and the spidroin secretory production levels (% total extracellular proteins). More specifically, both the protein concentrations and secretory production levels were determined by the Bradford assay and SDS-PAGE gel colorimetric method, both of which rely on Coomassie blue staining (see methods for details). According to Fahnestock and Bedzyk (1997), Coomassie binding to recombinant spidroin is only 7.5% as efficient as its binding to the standard protein bovine serum albumin, and hence the amount of spidroin is underrepresented relative to the endogenous contaminant proteins of the production host. Consequently, the extracellular spidroin titers presented above can be considered as minimum values (i.e., they are underestimated). To evaluate the degree of underestimation, the water solution of the purified MaSpI16 was lyophilized to a constant mass, leading to the purification titer of 2165 ± 124 mg L^{-1} culture supernatant. In view of the purity (93.0%) and recovery yield (84.9%) of the purification process (Fig. 4B), the actual secretion titer of MaSpI16 is estimated to be 2371 mg L^{-1} at the end of fermentation; the above Coomassie staining-based secretion titer was underestimated by approximately 4.3-fold. Nonetheless, for the purpose of monitoring the time profiles of the fed-batch HCDC, it would be more practical to present the secretion titers based on Coomassie staining.

So far, *E. coli* is one of the most widely studied host for intracellular production of recombinant spider dragline silk proteins in our and other groups (e.g., Bowen et al., 2018; Hu et al., 2021; Saric et al., 2021; Schmuck et al., 2021; Xia et al., 2010). For parallel comparison, we also expressed and purified a recombinant spidroin termed I16 in *E. coli*, which was composed of 16 consensus repeats of the major ampullate spidroin 1 of spider *T. clavipes* as described in our recent study (Hu et al., 2021). The results in Fig. S10 revealed that this spidroin had similar secondary structures, monodispersity and aggregation states as its *C. glutamicum* counterpart (MaSpI16). However, the aqueous solubility of I16 (34%, w/v) was approximately twofold lower than the secreted spidroin MaSpI16 (66%). Furthermore, the I16 fibers derived from 30% dope (the maximal operational concentration for spinning) were similar in strength and stiffness yet inferior in extensibility and toughness as compared to the MaSpI16 HD fibers from *C. glutamicum*. Besides easy purification, the above observations highlight additional merits of secretory spidroin production.

In conclusion, we have developed engineered *C. glutamicum* strains for the high-level secretory production of recombinant spider dragline silk proteins. Moreover, we provide a consolidated procedure for the chromatography-free purification of the secreted spidroins and preparation of aqueous dopes that can be directly spun into synthetic water-insoluble fibers with appreciable mechanical properties. As many other proteinaceous materials such as elastin and resilin are also derived from repetitive proteins with disordered structures (Qian et al., 2020), the secretory *C. glutamicum* platform developed here will be useful for their secretory production. Thus, this work adds proteinaceous biopolymers (other than traditional folded fluorescent proteins and enzymes) into the range of recombinant proteins that can be secreted from the Gram-positive workhorse.

Author statement

Z.-G.Q. and X.-X.X. conceived, designed, and supervised the study. Q. J. performed bacterial strain construction and evaluation experiments, F.P. performed fiber spinning and characterization experiments, and participated in signal peptide screening. Q.J., F.P., C.-F.H., S.Y.L., Z.-G. Q., and X.-X.X. analyzed data. Q.J., F.P., S.Y.L., Z.-G.Q., and X.-X.X. wrote the manuscript with input from all authors.

Declaration of competing interest

A patent application has been filed to cover the technology reported in this work.

Acknowledgements

Financial support was provided by the National Key Research and Development Program of China (Grant No. 2020YFA0907702), the National Natural Science Foundation of China (Grant Nos. 22075179 and 32071414), and the Natural Science Foundation of Shanghai (21ZR1432100). X.-X.X also acknowledges the program for professor special appointment at Shanghai institutions of higher learning. We

thank Prof. Ningyi Zhou (Shanghai Jiao Tong University) for providing *C. glutamicum* RES167 and plasmids pXMJ19, and Prof. Guo-Qiang Chen (Tsinghua University) for providing plasmid pTRCmob.

Appendix A. Supplementary data

Supplementary data to this article can be found online at https://doi.org/10.1016/j.ymben.2022.01.009.

References

An, S.J., Yim, S.S., Jeong, K.J., 2013. Development of a secretion system for the production of heterologous proteins in *Corynebacterium glutamicum* using the Porin B signal peptide. Protein Expr. Purif 89, 251–257. https://doi.org/10.1016/j.pep.2013.04.003.

Andersson, M., Jia, Q., Abella, A., Lee, X.Y., Landreh, M., Purhonen, P., Hebert, H., Tenje, M., Robinson, C.V., Meng, Q., Plaza, G.R., Johansson, J., Rising, A., 2017. Biomimetic spinning of artificial spider silk from a chimeric minispidroin. Nat. Chem. Biol. 13, 262–264. https://doi.org/10.1038/nchembio.2269.

Ayoub, N.A., Garb, J.E., Tinghitella, R.M., Collin, M.A., Hayashi, C.Y., 2007. Blueprint for a high-performance biomaterial: full-length spider dragline silk genes. PLoS One 2, e514. https://doi.org/10.1371/journal.pone.0000514.

Azam, A., Li, C., Metcalf, K.J., Tullman-Ercek, D., 2016. Type III secretion as a generalizable strategy for the production of full-length biopolymer-forming proteins. Biotechnol. Bioeng. 113, 2313–2320. https://doi.org/10.1002/bit.25656.

Becker, J., Rohles, C.M., Wittmann, C., 2018. Metabolically engineered *Corynebacterium glutamicum* for bio-based production of chemicals, fuels, materials, and healthcare products. Metab. Eng. 50, 122–141. https://doi.org/10.1016/j.ymben.2018.07.008.

Bhattacharyya, G., Oliveira, P., Krishnaji, S.T., Chen, D., Hinman, M., Bell, B., Harris, T. I., Ghazitabatabaei, A., Lewis, R.V., Jones, J.A., 2021. Large scale production of synthetic spider silk proteins in *Escherichia coli*. Protein Expr. Purif. 183, 105839. https://doi.org/10.1016/j.pep.2021.105839.

Billman-Jacobe, H., Wang, L., Kortt, A., Stewart, D., Radford, A., 1995. Expression and secretion of heterologous proteases by *Corynebacterium glutamicum*. Appl. Environ. Microbiol. 61, 1610–1613. https://doi.org/10.1128/aem.61.4.1610-1613.1995.

Blackledge, T.A., Cardullo, R.A., Hayashi, C.Y., 2005. Polarized light microscopy, variability in spider silk diameters, and the mechanical characterization of spider silk. Invertebr. Biol. 124, 165–173. https://doi.org/10.1111/j.1744-7410.2005.00016.x.

Bowen, C.H., Dai, B., Sargent, C.J., Bai, W., Ladiwala, P., Feng, H., Huang, W., Kaplan, D. L., Galazka, J.M., Zhang, F., 2018. Recombinant spidroins fully replicate primary mechanical properties of natural spider silk. Biomacromolecules 19, 3853–3860. https://doi.org/10.1021/acs.biomac.8b00980.

Candelas, G.C., Arroyo, G., Carrasco, C., Dompenciel, R., 1990. Spider silkglands contain a tissue-specific alanine tRNA that accumulates *in vitro* in response to the stimulus for silk protein synthesis. Dev. Biol. 140, 215–220. https://doi.org/10.1016/0012-1606(90)90069-U.

Candelas, G., Candelas, T., Ortiz, A., Rodriguez, O., 1983. Translational pauses during a spider fibroin synthesis. Biochem. Biophys. Res. Commun. 116, 1033–1038. https://doi.org/10.1016/S0006-291X(83)80246-0.

Cao, H., Parveen, S., Ding, D., Xu, H., Tan, T., Liu, L., 2017. Metabolic engineering for recombinant major ampullate spidroin 2 (MaSp2) synthesis in *Escherichia coli*. Sci. Rep. 7, 11365. https://doi.org/10.1038/s41598-017-11845-2.

Chen, X., Knight, D.P., Vollrath, F., 2002. Rheological characterization of *Nephila* spidroin solution. Biomacromolecules 3, 644–648. https://doi.org/10.1021/bm0156126.

Cheng, F., Yu, H., Stephanopoulos, G., 2019. Engineering *Corynebacterium glutamicum* for high-titer biosynthesis of hyaluronic acid. Metab. Eng. 55, 276–289. https://doi.org/10.1016/j.ymben.2019.07.003.

Cho, J.S., Choi, K.R., Prabowo, C.P.S., Shin, J.H., Yang, D., Jang, J., Lee, S.Y., 2017. CRISPR/Cas9-coupled recombineering for metabolic engineering of *Corynebacterium glutamicum*. Metab. Eng. 42, 157–167. https://doi.org/10.1016/j.ymben.2017.06.010.

Chung, H., Kim, T.Y., Lee, S.Y., 2012. Recent advances in production of recombinant spider silk proteins. Curr. Opin. Biotechnol. 23, 957–964. https://doi.org/10.1016/j.copbio.2012.03.013.

Copeland, C.G., Bell, B.E., Christensen, C.D., Lewis, R.V., 2015. Development of a process for the spinning of synthetic spider silk. ACS Biomater. Sci. Eng. 1, 577–584. https://doi.org/10.1021/acsbiomaterials.5b00092.

Fahnestock, S.R., Bedzyk, L.A., 1997. Production of synthetic spider dragline silk protein in *Pichia pastoris*. Appl. Microbiol. Biotechnol. 47, 33–39. https://doi.org/10.1007/s002530050884.

Foong, C.P., Higuchi-Takeuchi, M., Malay, A.D., Oktaviani, N.A., Thagun, C., Numata, K., 2020. A marine photosynthetic microbial cell factory as a platform for spider silk production. Commun. Biol. 3, 357. https://doi.org/10.1038/s42003-020-1099-6.

Freudl, R., 2018. Signal peptides for recombinant protein secretion in bacterial expression systems. Microb. Cell Factories 17, 52. https://doi.org/10.1186/s12934-018-0901-3.

Gatesy, J., Hayashi, C., Motriuk, D., Woods, J., Lewis, R., 2001. Extreme diversity, conservation, and convergence of spider silk fibroin sequences. Science 291, 2603–2605. https://doi.org/10.1126/science.1057561.

Gonska, N., López, P.A., Lozano-Picazo, P., Thorpe, M., Guinea, G.V., Johansson, J., Barth, A., Pérez-Rigueiro, J., Rising, A., 2020. Structure–function relationship of artificial spider silk fibers produced by straining flow spinning. Biomacromolecules 21, 2116–2124. https://doi.org/10.1021/acs.biomac.0c00100.

Hansmeier, N., Chao, T.C., Pühler, A., Tauch, A., Kalinowski, J., 2006. The cytosolic, cell surface and extracellular proteomes of the biotechnologically important soil bacterium *Corynebacterium efficiens* YS-314 in comparison to those of *Corynebacterium glutamicum* ATCC 13032. Proteomics 6, 233–250. https://doi.org/10.1002/pmic.200500144.

Heim, M., Keerl, D., Scheibel, T., 2009. Spider silk: from soluble protein to extraordinary fiber. Angew. Chem. Int. Ed. 48, 3584–3596. https://doi.org/10.1002/anie.200803341.

Hermann, T., Pfefferle, W., Baumann, C., Busker, E., Schaffer, S., Bott, M., Sahm, H., Dusch, N., Kalinowski, J., Pühler, A., Bendt, A.K., Krämer, R., Burkovski, A., 2001. Proteome analysis of *Corynebacterium glutamicum*. Electrophoresis 22, 1712–1723. https://doi.org/10.1002/1522-2683(200105)22:9<1712::AID-ELPS1712>3.0.CO;2-G.

Hijirida, D.H., Do, K.G., Michal, C., Wong, S., Zax, D., Jelinski, L.W., 1996. ^{13}C NMR of *Nephila clavipes* major ampullate silk gland. Biophys. J. 71, 3442–3447. https://doi.org/10.1016/S0006-3495(96)79539-5.

Holland, C., Terry, A.E., Porter, D., Vollrath, F., 2006. Comparing the rheology of native spider and silkworm spinning dope. Nat. Mater. 5, 870–874. https://doi.org/10.1038/nmat1762.

Houssin, C., de Sousa d'Auria, C., Constantinesco, F., Dietrich, C., Labarre, C., Bayan, N., 2020. Architecture and biogenesis of the cell envelope of Corynebacterium glutamicum. In: Inui, M., Toyoda, K. (Eds.), *Corynebacterium glutamicum*: Biology and Biotechnology. Springer, Cham, pp. 25–60. https://doi.org/10.1007/978-3-030-39267-3_2.

Hu, C.F., Qian, Z.G., Peng, Q., Zhang, Y., Xia, X.X., 2021. Unconventional spidroin assemblies in aqueous dope for spinning into tough synthetic fibers. ACS Biomater. Sci. Eng. 7, 3608–3617. https://doi.org/10.1021/acsbiomaterials.1c00492.

Hu, X., Kaplan, D., Cebe, P., 2006. Determining beta-sheet crystallinity in fibrous proteins by thermal analysis and infrared spectroscopy. Macromolecules 9, 6161–6170. https://doi.org/10.1021/ma0610109.

Huemmerich, D., Scheibel, T., Vollrath, F., Cohen, S., Gat, U., Ittah, S., 2004. Novel assembly properties of recombinant spider dragline silk proteins. Curr. Biol. 14, 2070–2074. https://doi.org/10.1016/j.cub.2004.11.005.

Jenkins, J.E., Creager, M.S., Lewis, R.V., Holland, G.P., Yarger, J.L., 2010. Quantitative correlation between the protein primary sequences and secondary structures in spider dragline silks. Biomacromolecules 11, 192–200. https://doi.org/10.1021/bm9010672.

Jones, J.A., Harris, T.I., Tucker, C.L., Berg, K.R., Christy, S.Y., Day, B.A., Gaztambide, D. A., Needham, N.J.C., Ruben, A.L., Oliveira, P.F., Decker, R.E., Lewis, R.V., 2015. More than just fibers: an aqueous method for the production of innovative recombinant spider silk protein materials. Biomacromolecules 16, 1418–1425. https://doi.org/10.1021/acs.biomac.5b00226.

Kikuchi, Y., Itaya, H., Date, M., Matsui, K., Wu, L.F., 2009. TatABC overexpression improves *Corynebacterium glutamicum* Tat-dependent protein secretion. Appl. Environ. Microbiol. 75, 603–607. https://doi.org/10.1128/AEM.01874-08.

Kono, N., Nakamura, H., Mori, M., Yoshida, Y., Ohtoshi, R., Malay, A.D., Pedrazzoli Moran, D.A., Tomita, M., Numata, K., Arakawa, K., 2021. Multicomponent nature underlies the extraordinary mechanical properties of spider dragline silk. Proc. Natl. Acad. Sci. U.S.A. 118, e2107065118 https://doi.org/10.1073/pnas.2107065118.

Kuwana, Y., Sezutsu, H., Nakajima, K., Tamada, Y., Kojima, K., 2014. High-toughness silk produced by a transgenic silkworm expressing spider (*Araneus ventricosus*) dragline silk protein. PLoS One 9, e105325. https://doi.org/10.1371/journal.pone.0105325.

Lazaris, A., Arcidiacono, S., Huang, Y., Zhou, J.F., Duguay, F., Chretien, N., Welsh, E.A., Soares, J.W., Karatzas, C.N., 2002. Spider silk fibers spun from soluble recombinant silk produced in mammalian cells. Science 295, 472–476. https://doi.org/10.1126/science.1065780.

Lewis, R.V., Hinman, M., Kothakota, S., Fournier, M.J., 1996. Expression and purification of a spider silk protein: a new strategy for producing repetitive proteins. Protein Expr. Purif. 7, 400–406. https://doi.org/10.1006/prep.1996.0060.

Liu, Q., Ouyang, S.P., Kim, J., Chen, G.Q., 2007. The impact of PHB accumulation on L-glutamate production by recombinant *Corynebacterium glutamicum*. J. Biotechnol. 132, 273–279. https://doi.org/10.1016/j.jbiotec.2007.03.014.

Liu, X., Yang, Y., Zhang, W., Sun, Y., Peng, F., Jeffrey, L., Harvey, L., McNeil, B., Bai, Z., 2015. Expression of recombinant protein using *Corynebacterium glutamicum*: progress, challenges and applications. Crit. Rev. Biotechnol. 36, 652–664. https://doi.org/10.3109/07388551.2015.1004519.

Matsuda, Y., Itaya, H., Kitahara, Y., Theresia, N.M., Kutukova, E.A., Yomantas, Y.A.V., Date, M., Kikuchi, Y., Wachi, M., 2014. Double mutation of cell wall proteins CspB and PBP1a increases secretion of the antibody Fab fragment from *Corynebacterium glutamicum*. Microb. Cell Factories 13, 56. https://doi.org/10.1186/1475-2859-13-56.

Metcalf, K.J., Finnerty, C., Azam, A., Valdivia, E., Tullman-Erceka, D., 2014. Using transcriptional control to increase titers of secreted heterologous proteins by the type III secretion system. Appl. Environ. Microbiol. 80, 5927–5934. https://doi.org/10.1128/AEM.01330-14.

Oktaviani, N.A., Matsugami, A., Malay, A.D., Hayashi, F., Kaplan, D.L., Numata, K., 2018. Conformation and dynamics of soluble repetitive domain elucidates the initial β-sheet formation of spider silk. Nat. Commun. 9, 2121. https://doi.org/10.1038/s41467-018-04570-5.

Omenetto, F.G., Kaplan, D.L., 2010. New opportunities for an ancient material. Science 329, 528–531. https://doi.org/10.1126/science.1188936.

Park, S.H., Kim, H.U., Kim, T.Y., Park, J.S., Kim, S.S., Lee, S.Y., 2014. Metabolic engineering of *Corynebacterium glutamicum* for L-arginine production. Nat. Commun. 5, 4618. https://doi.org/10.1038/ncomms5618.

Qian, Z.G., Zhou, M.L., Song, W.W., Xia, X.X., 2015. Dual thermosensitive hydrogels assembled from the conserved C-terminal domain of spider dragline silk. Biomacromolecules 16, 3704–3711. https://doi.org/10.1021/acs.biomac.5b01231.

Qian, Z.G., Pan, F., Xia, X.X., 2020. Synthetic biology for protein-based materials. Curr. Opin. Biotechnol. 65, 197–204. https://doi.org/10.1016/j.copbio.2020.04.004.

Qin, N., Qian, Z.G., Zhou, C., Xia, X.X., Tao, T.H., 2021. 3D electron-beam writing at sub-15 nm resolution using spider silk as a resist. Nat. Commun. 12, 5133. https://doi.org/10.1038/s41467-021-25470-1.

Rousseau, M.E., Lefèvre, T., Pézolet, M., 2009. Conformation and orientation of proteins in various types of silk fibers produced by *Nephila clavipes* spiders. Biomacromolecules 10, 2945–2953. https://doi.org/10.1021/bm9007919.

Saric, M., Eisoldt, L., Döring, V., Scheibel, T., 2021. Interplay of different major ampullate spidroins during assembly and implications for fiber mechanics. Adv. Mater. 33, 2006499. https://doi.org/10.1002/adma.202006499.

Schäfer, A., Tauch, A., Jäger, W., Kalinowski, J., Thierbach, G., Pühler, A., 1994. Small mobilizable multi-purpose cloning vectors derived from the *Escherichia coli* plasmids pK18 and pK19: selection of defined deletions in the chromosome of *Corynebacterium glutamicum*. Gene 145, 69–73. https://doi.org/10.1016/0378-1119(94)90324-7.

Scheller, J., Gührs, K.H., Grosse, F., Conrad, U., 2001. Production of spider silk proteins in tobacco and potato. Nat. Biotechnol. 19, 573–577. https://doi.org/10.1038/89335.

Schmuck, B., Greco, G., Barth, A., Pugno, N.M., Johansson, J., Rising, A., 2021. High-yield production of a super-soluble miniature spidroin for biomimetic high-performance materials. Mater. Today 50, 16–23. https://doi.org/10.1016/j.mattod.2021.07.020.

Swanson, B.O., Blackledge, T.A., Summers, A.P., Hayashi, C.Y., 2006. Spider dragline silk: correlated and mosaic evolution in high-performance biological materials. Evolution 60, 2539–2551. https://doi.org/10.1111/j.0014-3820.2006.tb01888.x.

Sponner, A., Schlott, B., Vollrath, F., Unger, E., Grosse, F., Weisshart, K., 2005. Characterization of the protein components of *Nephila clavipes* dragline silk. Biochemistry 44, 4727–4736. https://doi.org/10.1021/bi047671k.

Teramoto, H., Watanabe, K., Suzuki, N., Inui, M., Yukawa, H., 2011. High yield secretion of heterologous proteins in *Corynebacterium glutamicum* using its own Tat-type signal sequence. Appl. Microbiol. Biotechnol. 91, 677–687. https://doi.org/10.1007/s00253-011-3281-8.

Teulé, F., Miao, Y.G., Sohn, B.H., Kim, Y.S., Hull, J.J., Fraser Jr., M.J., Lewis, R.V., Jarvis, D.L., 2012. Silkworms transformed with chimeric silkworm/spider silk genes spin composite silk fibers with improved mechanical properties. Proc. Natl. Acad. Sci. U.S.A. 109, 923–928. https://doi.org/10.1073/pnas.1109420109.

Watanabe, K., Tsuchida, Y., Okibe, N., Teramoto, H., Suzuki, N., Inui, M., Yukawa, H., 2009. Scanning the *Corynebacterium glutamicum* R genome for high-efficiency secretion signal sequences. Microbiology 155, 741–750. https://doi.org/10.1099/mic.0.024075-0.

Watanabe, K., Teramoto, H., Suzuki, N., Inui, M., Yukawa, H., 2013. Influence of SigB inactivation on *Corynebacterium glutamicum* protein secretion. Appl. Microbiol. Biotechnol. 97, 4917–4926. https://doi.org/10.1007/s00253-012-4586-y.

Weatherbee-Martin, N., Xu, L., Hupe, A., Kreplak, L., Fudge, D.S., Liu, X.Q., Rainey, J.K., 2016. Identification of wet-spinning and post-spin stretching methods amenable to recombinant spider aciniform silk. Biomacromolecules 17, 2737–2746. https://doi.org/10.1021/acs.biomac.6b00857.

Wei, S.P., Qian, Z.G., Hu, C.F., Pan, F., Chen, M.T., Lee, S.Y., Xia, X.X., 2020. Formation and functionalization of membraneless compartments in *Escherichia coli*. Nat. Chem. Biol. 16, 1143–1148. https://doi.org/10.1038/s41589-020-0579-9.

Whittall, D.R., Baker, K.V., Breitling, R., Takano, E., 2021. Host systems for the production of recombinant spider silk. Trends Biotechnol. 39, 560–573. https://doi.org/10.1016/j.tibtech.2020.09.007.

Widmaier, D.M., Tullman-Ercek, D., Mirsky, E.A., Hill, R., Govindarajan, S., Minshull, J., Voigt, C.A., 2009. Engineering the *Salmonella* type III secretion system to export spider silk monomers. Mol. Syst. Biol. 5, 309. https://doi.org/10.1038/msb.2009.62.

Winkler, S., Wilson, D., Kaplan, D.L., 2000. Controlling β-sheet assembly in genetically engineered silk by enzymatic phosphorylation/dephosphorylation. Biochemistry 39, 12739–12746. https://doi.org/10.1021/bi001335w.

Xia, X.X., Qian, Z.G., Ki, C.S., Park, Y.H., Kaplan, D.L., Lee, S.Y., 2010. Native-sized recombinant spider silk protein produced in metabolically engineered *Escherichia coli* results in a strong fiber. Proc. Natl. Acad. Sci. U.S.A. 107, 14059–14063. https://doi.org/10.1073/pnas.1003366107.

Xu, J., Dong, Q., Yu, Y., Niu, B., Ji, D., Li, M., Huang, Y., Chen, X., Tan, A., 2018. Mass spider silk production through targeted gene replacement in *Bombyx mori*. Proc. Natl. Acad. Sci. U.S.A. 115, 8757–8762. https://doi.org/10.1073/pnas.1806805115.

Xu, G., Zha, J., Cheng, H., Ibrahim, M.H.A., Yang, F., Dalton, H., Cao, R., Zhu, Y., Fang, J., Chi, K., Zheng, P., Zhang, X., Shi, J., Xu, Z., Gross, R.A., Koffas, M.A.G., 2019. Engineering *Corynebacterium glutamicum* for the *de novo* biosynthesis of tailored poly-γ-glutamic acid. Metab. Eng. 56, 39–49. https://doi.org/10.1016/j.ymben.2019.08.011.

Yang, Y.X., Qian, Z.G., Zhong, J.J., Xia, X.X., 2016. Hyper-production of large proteins of spider dragline silk MaSp2 by *Escherichia coli* via synthetic biology approach. Process Biochem. 51, 484–490. https://doi.org/10.1016/j.procbio.2016.01.006.

Yarger, J.L., Cherry, B.R., van der Vaart, A., 2018. Uncovering the structure-function relationship in spider silk. Nat. Rev. Mater. 3, 18008. https://doi.org/10.1038/natrevmats.2018.8.

Yim, S.S., Choi, J.W., Lee, R.J., Lee, Y.J., Lee, S.H., Kim, S.Y., Jeong, K.J., 2016. Development of a new platform for secretory production of recombinant proteins in *Corynebacterium glutamicum*. Biotechnol. Bioeng. 113, 163–172. https://doi.org/10.1002/bit.25692.

Zhang, Y., Hu, J., Miao, Y., Zhao, A., Zhao, T., Wu, D., Liang, L., Miikura, A., Shiomi, K., Kajiura, Z., Nakagaki, M., 2008. Expression of EGFP-spider dragline silk fusion protein in BmN cells and larvae of silkworm showed the solubility is primary limit for dragline proteins yield. Mol. Biol. Rep. 35, 329–335. https://doi.org/10.1007/s11033-007-9090-6.

Zhou, Z., Zhang, S., Cao, Y., Marelli, B., Xia, X.X., Tao, T.H., 2018. Engineering the future of silk materials through advanced manufacturing. Adv. Mater. 30, 1706983. https://doi.org/10.1002/adma.201706983.